Simulation Test of the Cutting Process

Dominik Wilczyński[0000-0003-1758-6063], *Krzysztof* Wałęsa[0000-0003-0651-4485], and *Aleksandra* Biszczanik[0000-0002-6765-7459]

Poznań University of Technology, Piotrowo Str. 3, Poznań, Poland

Abstract. Cutting is a production process commonly employed used in various industries. The aim of improving its efficiency entails the improvement of the durability of the cutting blade, increasing the accuracy in terms of the resulting item dimensions obtained after cutting, but also the quality of the obtained edge. The material factor for the above is the distribution of forces in the cutting edge and cut element system. Furthermore, the pursuit of minimized interaction of forces in this process is of significance, which has a positive impact both on the durability of the blade as well as the process energy consumption. The paper presents a simulation of the process of cutting a flat bar made of aluminium. The numerical model was built in the ABAQUS system. The model includes a knife-cut element. The purpose of performing simulation tests is to determine the cutting force, changes in its value and the nature of these changes when cutting with knives of different geometry and trajectory.

1 Introduction

Aluminum is a widely utilized material due to its universal application in construction. Presently, many researchers study the process of cutting this material employing various techniques, e.g..: laser cutting [1] or water jet cutting [2].
The present paper presents the methodology and results of simulation studies of the process of cutting aluminum sheets of different thickness using knives of various blade geometry. The aim of the research is to identify the lowest possible force required to cut the item.

Cutting as a technological process is utilized in many areas of the economy and studied by many researchers worldwide[3-5].Part of this research effort focuses on the process of cutting (breaking down)biomass, which is necessary to achieve the desired particle size, significantly affecting the process of compaction and the characteristics of the resultant biofuel. Many researchers focus on analyzing the effect of the characteristics of cut biomass as well as the parameters of the cutting implement [6-13]in terms of achieving the lowest possible energy consumption of the process being a prerequisite stage of the compaction process(the process employed to compact different types of materials [14-20]), which is a factor in the total energy input required to obtained biofuel with good energy characteristics. Another object of research is the degree of compaction of the bone structure in the process of hip bone implant fixation for the purpose of identifying the suitable force to carry out the process [21, 22].Another relevant subject of interest is the study of the

influence of the individual controls and operating subassemblies of the compacting device which have a material influence on the process quality and energy consumption [23-26].

2 Simulation Model

The numerical model was developed in the Abaqus system comprising a knife and the aluminum item to be cut. The cut item is rectangular shaped with three different thickness values: 0.1 mm, 0.5 mm and 1 mm, whereas the knife is represented by a steel component with shaped blade geometry (see Fig. 1a and 1b).
The simulation examines the influence of the knife rake angle α (5°, 15°, 30°), the knife blade angle β (0°, 30°, 45° and 60°) as well as the thickness of the cut item on the force value necessary to cut it.For the given value of rake angle α, four knives were modeled with four values of the blade angle β equal to: 0°, 30°, 45° and 60° (see Fig. 1).The simulation was carried out for each possible combination of angles α and β as well as the cut item width of 0.1 mm. In total, 12simulations were carried out. Afterwards, the angle values α and β were selected in which the measured cutting force was the lowest and for these cases of blade geometry further simulations were carried out, cutting samples with thickness equal to 0.5 and 1 mm. Consequently, six more simulations were performed,up to 18 simulations in total.
In the simulation, all the degrees of freedom for the extreme ends of the cut sample were restrained as well as for the nodes at the distance equal to four lengths of the finite element away from the knife edge (see Fig. 1a).

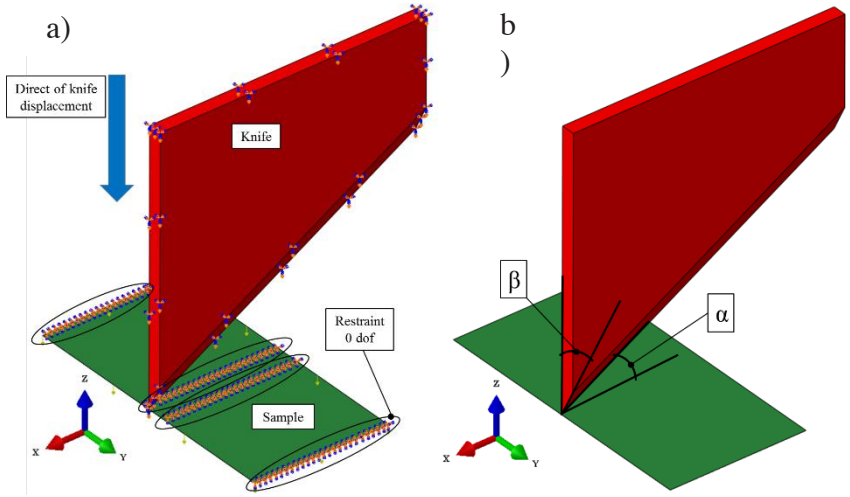

Fig. 1. General view of the system model for the knife - cut element: a) with indication of assumed boundary conditions for the simulation, b) with indication of the knife blade geometry parameter designations.

The model of the knife and sample accounts for gravity, whereas the knife displacement is forced as a motion along the Z axis (see Fig. 1a).
The knife model characteristics are equal to steel material, whereas the cut sample assumes characteristics of aluminum including the Johnson-Cook damage model parameters as provided below in Table 1 [27, 28].

Table 1. Johnson-Cook damage model parameters [27, 28].

d1	d2	d3	d4	d5	Melting Temperature	Melting Temperature	Reference Strain Rate
-0.77	1.45	0.47	0.001	0	0	0	1

The knife and sample models were discretized using a hexahedron mesh with reduced integration to single point – type C3D8R, as shown on Fig. 2.

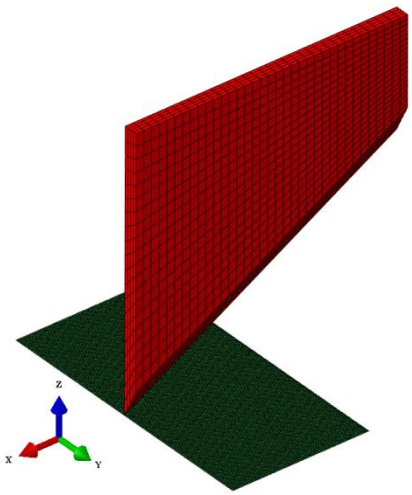

Fig. 2. General view of the discretized model of the knife and cut sample.

3 Simulation Tests and Results

The below Figures (see Fig. 3a-3d)present example results of the simulation for selected knife blade geometries.

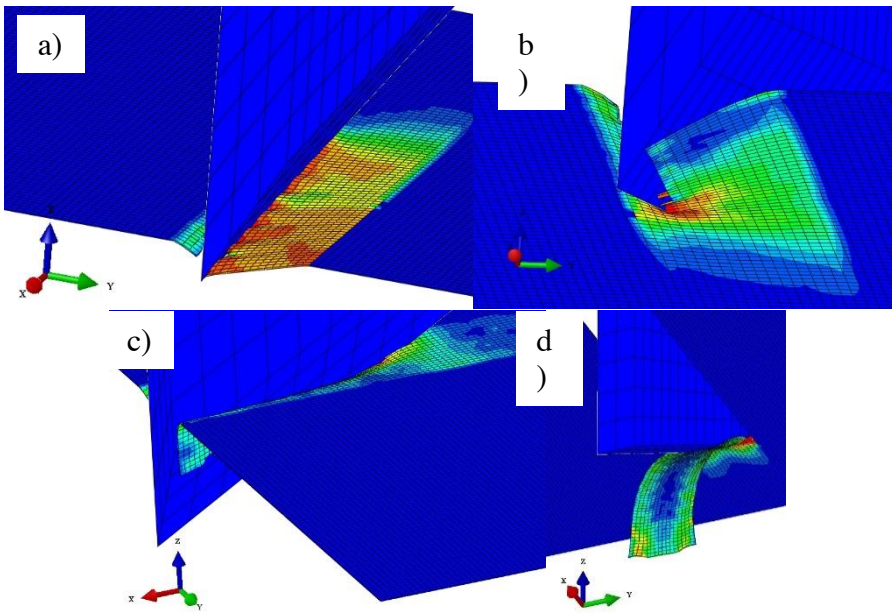

Fig. 3. General view of the phases of the cutting process simulation for the following cases: a) back-rake angle α = 5°, blade angle β = 60°, b) back-rake angle α = 15°, blade angle β = 60°, c) back-rake angle α = 30°, blade angle β = 60°, d)) back-rake angle α = 30°, blade angle β = 0°.

Fig. 4 demonstrates an example graph line indicating the variance of force value in the course of the simulation for angle values α = 30°and β = 30°.

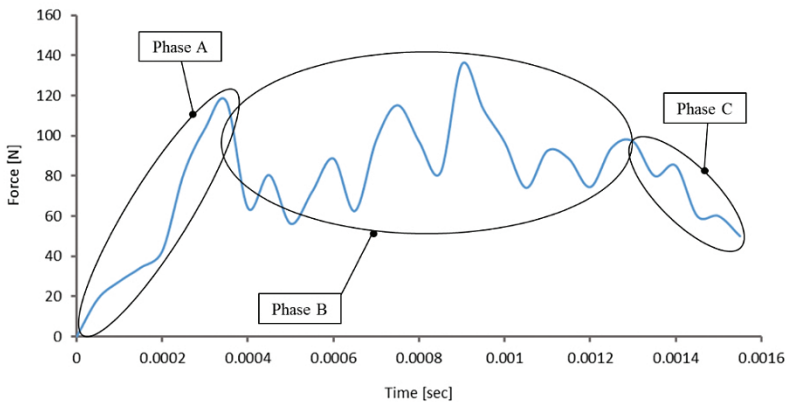

Fig. 4. Example characteristic of cutting force variance in the course of the simulation for angle values α = 30°and β = 30°.

Analyzing the change in cutting force value (see Fig. 4),it is possible to identify three distinct phases in its graph line. The first phase A corresponds to the knife blade initial penetration of the material. In this stage, a sudden increase in the cutting force value is observed, accompanied by the severance of the material structure.Phase B corresponds to the blade displacement within the material. In this phase,the force value varies within the

defined range. This is affected by variable resistance to motion between the knife blade and the cut material resulting from the changing area of contact between surfaces. The last Phase C corresponds to the blade exiting the material, characterized by a distinct decrease in force value.Figures 5, 6 and 7show the breakdown of the characteristics of cutting force variance for specific values of the rake angle and blade angle with the cut sample thickness of 0.1 mm.

Fig. 5 shows the variance of the cutting force graph line in time for the rake angle value α = 5°and blade geometry angles β = 30°, 45° and 60°. With the change of value of the blade inclination angle from 30° to 45°, a decrease in the cutting force value is observed. The increase of the angle to 60° causes the cutting force to increase.The smooth graph line for the cutting force variance is achieved with the blade angle of β = 0°,this is caused by the interaction of two cutting edges throughout the entire process (see Fig. 3d). The cutting force value in this case is lower in comparison to the force value during cutting with the blade angles β = 30° and 60°.

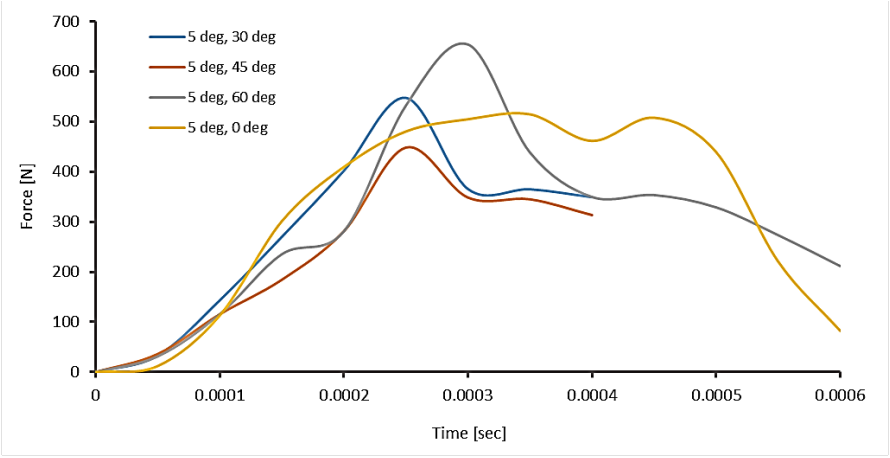

Fig. 5. Characteristics of the cutting force variance in the course of the simulation for angle values α = 5° and β = 0°, 30°, 45° and 60° with cut sample thickness of 0.1 mm.

Fig. 6 demonstrates the graph line for the cutting force variance for the rake angle value of α = 15°. The graph demonstrates a declining tendency for the force value together with the increase in the knife blade angle, being the most noticeable for angle value β = 60°.The graph line for the cutting force at blade angle β = 0° is to be analyzed separately, demonstrating a smoother line in comparison to the other cases. With the increase of the rake angle from 5° to 15°,a significant decrease in the cutting force value is observed for all blade angle values β.

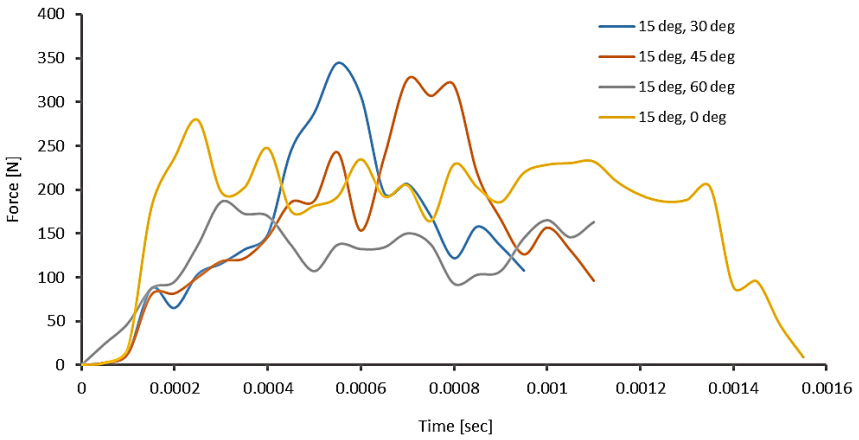

Fig. 6. Characteristics of the cutting force variance in the course of the simulation for angle values α = 15° and β = 0°, 30°, 45° and 60°with cut sample thickness of 0.1 mm.

With the increase of rake angle to α = 30° (see Fig. 7) a significant decrease of the cutting force value is also observed for all values of angle β. Furthermore, a tendency is observed for the decrease in the force value together with the increase of the angle value β. Contrary to the other, earlier cases, the highest cutting force value was registered for the angle value β = 0°.

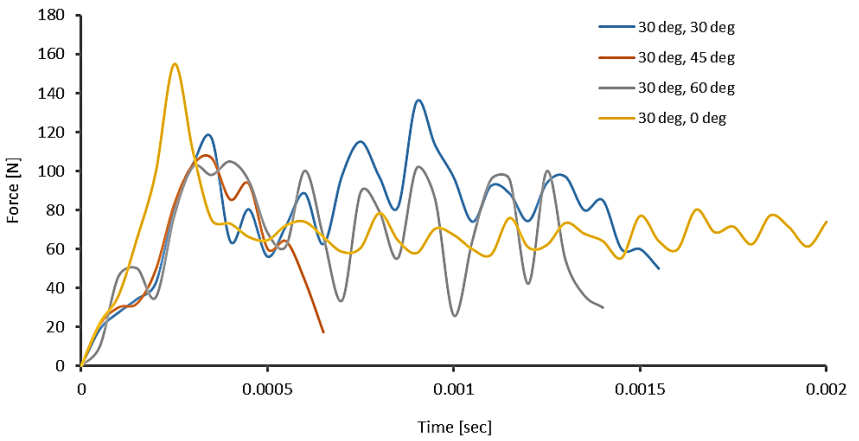

Fig. 7. Characteristics of the cutting force variance in the course of the simulation for angle values α = 30° and β = 0°, 30°, 45° and 60° with cut sample thickness of 0.1 mm.

Table 2 lists the maximum force values in the course of the cutting process for specific values of angles α and β.

Table 2. List of maximum force values registered in the course of the process simulation for cutting the 0.1 mm thick sampletogether with specific values of angles α and β.

α i β [deg]	Max force value [N]	α i β [deg]	Max force value [N]
5 deg, 30 deg	547.2	15 deg, 60 deg	186
5 deg, 45 deg	448.2	15 deg, 0 deg	279.4
5 deg, 60 deg	653.9	30 deg, 30 deg	135.6
5 deg, 0 deg	514.5	30 deg, 45 deg	106.8
15 deg, 30 deg	344.5	30 deg, 60 deg	105
15 deg, 45 deg	325.9	30 deg, 0 deg	155

The lowest cutting force values were registered for the rake angle α = 30° and blade angles β = 30°, 45° and 60°,therefore further simulations were carried outfor these values of angles α and βin order to determine the influence of sample thickness on the value of cutting force necessary to separate the material.Figures 8 and 9 show the graph lines indicating the variance of the cutting force for sample thicknesses 0.5 mm and 1 mm.
With the increase of thickness of the cut material, the cutting force increases severalfold;during phase B of the cutting process, a momentary increase in force is observe, resulting from significant resistances to motion of the penetrating knife blade. For both cases of increased sample thickness, a tendency is observed for the cutting force value to increase in phases A and B of the cutting process together with the increase of the value of the angle β.

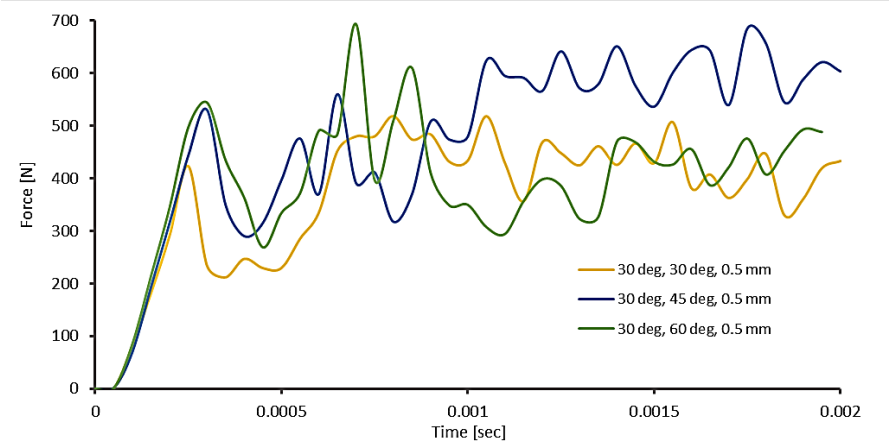

Fig. 8. Characteristics of the cutting force variance as a function of different values of angles α and β with cut sample thickness equal to 0.5 mm.

The force value in phase A is lower than in phase B as the entire blade which initializes the separation of the sample material does not come into contact with its edges formed by the separation. In phase B the resistances to motion increase as in addition to cutting the material it is necessary to overcome the resistance forces resultant from the knife blade's contact with the newly formed edges.

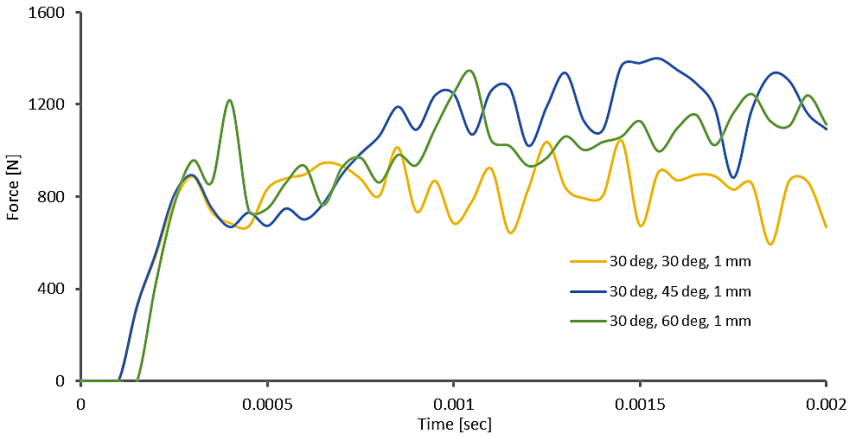

Fig. 9. Characteristics of the cutting force variance as a function of different values of angles α and β with cut sample thickness equal to 1 mm.

What follows from analyzing the registered graph lines (see Fig. 9), is that the force required to separate the material (phase A)is the same for angle values β = 30° and 45°. In the following stage of the process (phase B) the force value increases noticeably for blade angles β = 45° and 60°. The observation is different for the blade angle β = 30°.
Additionally, a process analysis was carried out for the knife motion along the X axis (see Fig. 10). The simulation was carried out for blade angles α =30° and β = 30°, α =30°and β = 45° α =30°and β = 60°. The thickness of the cut material was 1 mm. Fig. 11 shows the general view of the simulation run for angles α = 30°, β = 45° and thickness of the cut material 1 mm.

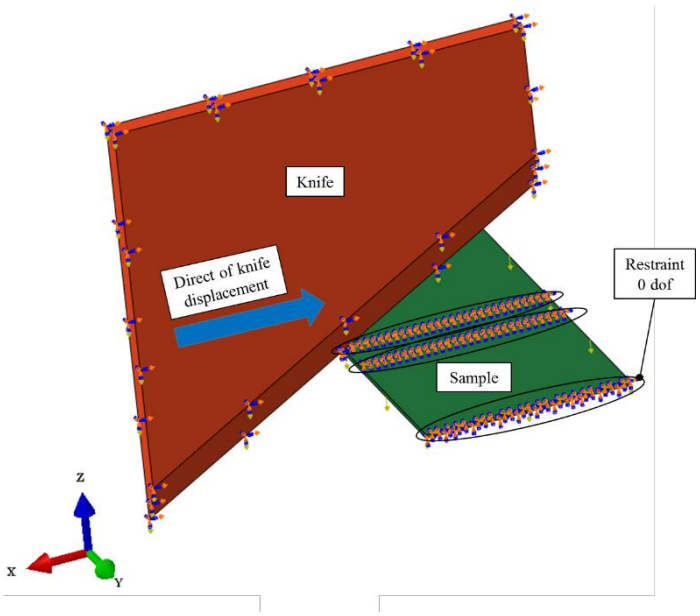

Fig. 10. General view of the system model for the knife and cut sample with the knife moving along the X axis.

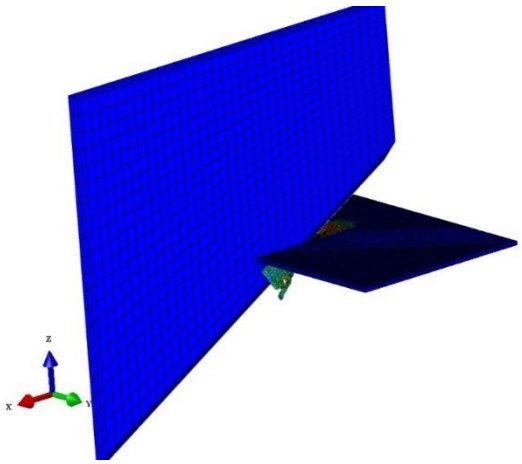

Fig. 11. General view of the model during the cutting process simulation with the knife moving along the X axis, with knife blade angles α = 30°, β = 45° and cut sample thickness 1 mm.

Fig. 12 shows the characteristics of cutting force variance for the analyzed knife motion along the X axis for blade angles α =30° and β = 30°, α =30°and β = 45°, α = 30° and β = 60° and cut sample thickness 1 mm.

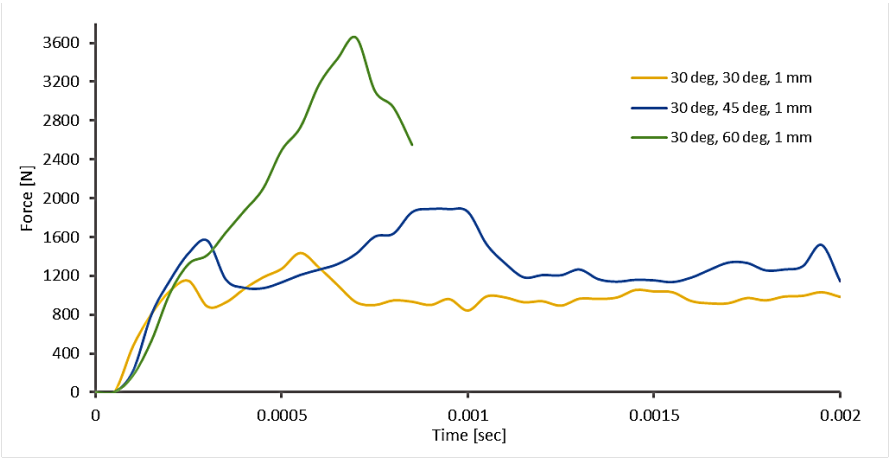

Fig. 12. Characteristics of variance of the cutting force as a function of varying angle values α and β for knife motion along the X axis and thickness of the cut sample equal to 1 mm.

Comparing the obtained results shown on Fig. 12relevant to the knife motion along the axis X with the results obtained for the knife motion along the axis Z, considering the same values of the knife blade angles, we observed general increase in cutting force value for respective values of angles α and β. The tendency to increase the cutting force together with the increase of the value of angle β is maintained. For the blade angle value β = 60° no clear indication of phase B of the cutting process is seen.

4 Conclusions

The following conclusions can be formulated based on the results of the performed simulation studies:

1. A significant factor on reducing the cutting force value is the rake angle α, its increase causes a noticeable decrease in the cutting force value.
2. With the increase of the rake angle value α,the total length of the knife blade penetrating the cut sample decreases which reduces the value of cutting force.
3. The effect of the value of the blade angle β on the cutting force is not significant when the knife is moving along the Z axis. When the knife moves along the X axis, the value of the blade angle β has a noticeable effect on the cutting force value.
4. The results obtained from the developed simulation model allow to select the optimal knife blade geometry; however, the simulation study should be supplemented by experimental studies to determine the simulation error value.

References

1. A. Stournaras, P. Stavropoulos, K., Salonitis, G. Chryssolouris An investigation of quality in CO2 laser cutting of aluminium. CIRP Journal of Manufacturing Science and Technology, 2, 61-69 (2009).
2. H.Y. Zheng, Z.Z. Han, Z.D. Chen, W.L. Chen, S. Yeo Quality and Cost.: Comparisons Between Laser and Waterjet Cutting. Journal of Materials Processing Technology, 62, 294-298 (1996).
3. D. Wojtkowiak, K. Talaśka The influence of the piercing punch profile on the stress distribution on its cutting edge. MATEC Web of Conferences, 254, 02001 (2019).
4. D. Wojtkowiak, K. Talaśka Determination of the effective geometrical features of the piercing punch for polymer composite belts. International Journal of Advanced Manufacturing Technology, 104, 1-4, 315-332 (2019).
5. D. Wojtkowiak, K. Talaśka, A. Fierek The application of the Finite Element Method analysis in the process of designing the punching die for belt perforation. IOP Conferences: Materials Science and Engineering, 776, 012057 (2020).
6. M. Azadbakht, E. Esmaeilzadeh, M. Esmaeili-Shayan Energy consumption during impact cutting of canola stalk as a function of moisture content and cutting height. Journal of the Saudi Society of Agricultural Sciences 14, 147-152 (2015).
7. S.K. Mathanker, T.E. Grift, A.C. Hansen Effect of blade oblique angle and cutting speed on cutting energy for energycane stems. Biosystems Engineering, 1331, 64-70 (2015).
8. D. Wilczyński, K. Talaśka, I., et al. Experimental research on biomass cutting process. MATEC Web of Conferences, 157, 07016 (2018).
9. D. Wilczyński, I. Malujda, J. Górecki, G. Domek Experimental research on the process of cutting transport belts. MATEC Web of Conferences, 254, 05014 (2019).
10. D. Wilczyński Multifactor analysis of experiment parameters on the example of the biomass cutting process. IOP Conference Series: Materials Science and Engineering, 776, 012013 (2020).
11. D. Wilczyński, K. Wałęsa, M. Berdychowski, M. Kukla Biomass cutting tests to determine the lowest value of the process force. IOP Conference Series: Materials Science and Engineering, 776, 012014 (2020).

12. Ł. Warguła, M. Kukla, P. Krawiec, B. Wieczorek Reduction in Operating Costs and Environmental Impact Consisting in the Modernization of the Low-Power Cylindrical Wood Chipper Power Unit by Using Alternative Fuel. Energies 13, 2995 (2020).
13. Ł. Warguła, P. Krawiec, K.J. Waluś, M. Kukla Fuel Consumption Test Results for a Self-Adaptive, Maintenance-Free Wood Chipper Drive Control System. Appl. Sci., 10, 2727 (2020).
14. J. Górecki, I. Malujda, K. Talaśka, et al.: Investigation of internal friction of agglomerated dry ice. Procedia Engineering, 136, 275-279 (2016).
15. J. Górecki, I. Malujda, K. Talaśka Influence of the Value of Limit densification Stress on the Quality of Pellets During the Agglomeration Process of CO2. Procedia Engineering, 136, 269-274 (2016).
16. J. Górecki, I. Malujda, K. Talaśka, et al. Dry ice compaction in piston extrusion process. Acta mechanica et automatica, 11, 4, 313-316 (2017).
17. J. Górecki, K. Talaśka, K. Wałęsa, D. Wilczyński, D. Wojtkowiak Mathematical Model Describing the Influence of Geometrical Parameters of Multichannel Dies on the Limit Force of Dry Ice Extrusion Process. Materials, 13, 15 (2020).
18. Berdychowski, M., Talaśka, K., Malujda, I., Kukla, M.: Application of the Mohr-Coulomb model for simulating the biomass compaction process. IOP Conference Series: Materials Science and Engineering, 776(1), 012066 (2020).
19. D. Wilczyński, I. Malujda, K. Talaśka, et al. The study of mechanical properties of natural polymers in the compacting process. Procedia Engineering, 177, 411-418 (2017).
20. K. Talaśka, I. Malujda, D. Wilczyński Agglomeration of natural fibrous materials in perpetual screw technique - a challenge for designer. Procedia Engineering, 136, 63-69 (2016).
21. M. Berdychowski, J. Mielniczuk, M. Matyjaszczyk Analysis of the Yield Condition of Porous Bone-implant Fixation. Procedia Engineering, 177, 358-362 (2017).
22. M. Berdychowski, J. Mielniczuk Analysis of the porous bone-implant fixation-experimental verification of numerical model. MATEC Web of Conferences, 157, 05002 (2018).
23. M. Dudziak, G. Domek, A. Kolodziej, et al. Contact Problems Between the Hub and the Shaft with a Three-Angular Shape of Cross-Section for Different Angular Positions. Procedia Engineering 96, 50-58 (2014).
24. M. Kukla, P. Tarkowski, I. Malujda, K. Talaśka, J. Górecki Determination of the torque characteristics of stepper motor. Procedia Engineering, 136, 375-379 (2016).
25. P. Tarkowski, I. Malujda, K. Talaśka, J. Górecki, M. Kukla Influence of the type of acceleration characteristic of the stepping motor for efficient power usage, Procedia Engineering, 136, 370-374 (2016).
26. D. Wojtkowiak, K. Talaśka, M. Berdychowski Analysis of the guiding column and sleeve cooperation in the linear slide bearing of the punching die head-punch block, IOP Conferences: Materials Science and Engineering, 776, 012055 (2020).
27. Abaqus Documentation.
28. I.S. Boldyrev, I.A. Shchurov, A.V. Nikonov Numerical simulation of the aluminum 6061-T6 cutting and the effect of the constitutive material model and failure criteria on cutting forces prediction. Procedia Engineering, 150, 866-870 (2016).